Insights into Zeolite-Supported Lanthanum Borohydride Catalyst in Benzene C–H Borylation by Solid-State NMR and Theoretical Calculations

Jinlei Cui,[1] Yuting Li,[1] Da-Jiang, Liu,[1] Marco Mais,[1] Jie Zhang,[1] Long Qi,[1] Aaron D. Sadow,[1,2] Takeshi Kobayashi[1]

[1] U.S. DOE Ames National Laboratory, Iowa State University, Ames, Iowa 50011, United States
2 Department of Chemistry, Iowa State University, Ames, Iowa 50011, United States

KEYWORDS: Solid-state NMR, machine-learning molecular dynamics, benzene C–H borylation, rare-earth organometallics, zeolite

Table of Contents

Chemicals and Materials

All chemicals were stored in N_2-filled MBraun glove box unless otherwise indicated. Tetrahydrofuran (THF), pentane, and toluene solvents were obtained from Sigma Aldrich, deoxygenated and dried using an IT PureSolv System, and stored over 3 Å molecular sieves. 4,4,5,5-Tetramethyl-1,3,2-dioxaborolane (HBpin, 97%), 4,4,5,5-tetramethyl-2-phenyl-1,3,2-dioxaborolane (PhBpin, 97%), chlorotriphenylsilane (Ph_3SiCl, 96%), chlorodiphenylmethylsilane ($Ph_2MeSiCl$, 98%), chlorotrimethylsilane (Me_3SiCl, 97%), trimethoxylbenzene (TMOB), sodium borohydride (99.99%), and *N*,*N*-dimethyl(trimethylsilyl)amine ($Me_3Si\text{-}NMe_2$) were purchased from Sigma Aldrich. $LaCl_3$ (99.9% anhydrous) was obtained from Strem. Benzene-d_6 and toluene-d_8 were stirred and heated at reflux over Na/K alloy and vacuum-transferred. Dichloromethane-d_2 was stirred over calcium hydride overnight and then distilled. HY_{30} (CBV760, Si/Al = 30) and HY_{15} (CBV 720, Si/Al = 15) were purchased from Zeolyst and treated at 500 °C for 5 h under a dynamic vacuum (10^{-4} mbar). Aerosil 380 was purchased from Evonik and heated at 550 ºC for 5 h under a dynamic vacuum (10^{-4} mbar). HY_{250} (390HUA, Si/Al = 250) and HY_{50} (385HUA, Si/Al = 50) were purchased from Tosoh and heated at 500 °C for 5 h under dynamic vacuum (10^{-4} mbar).

Characterization Methods and Technologies

^1H and ^{11}B NMR spectra were measured on a Bruker Avance NEO-400 spectrometer. Gas chromatography-mass spectrometry (GC-MS) was performed using an Agilent 7890A GC and 5975C MS, equipped with a capillary Agilent J&W DB-5ht column.

Inductively coupled plasma - optical emission spectrometry (ICP-OES) analysis was performed using an Agilent 5800 to determine elemental composition (wt %) of lanthanum, boron/lanthanum ratio, and silicon/aluminum ratio in the catalysts.

N_2 physisorption measurements were performed using a Micromeritics TriStar surface characterization analyzer at 77 K to obtain surface area and pore volume of zeolitic supports with/without functionalization.

Transmission infrared spectroscopy or diffuse reflectance infrared Fourier transform spectroscopy (DRIFTS) experiments were conducted using a Bruker VERTEX 80 IR spectrometer equipped with a Harrick "Praying Mantis" accessory, and spectra of samples were recorded within the 4000-400 cm^{-1} wavenumber range. Samples were prepared in the glovebox under N_2 and sealed before measurements.

Powder X-ray diffraction (XRD) was conducted on a Bruker D8 ADVANCE diffractometer employed the LYNXEYE position-sensitive detector, using Cu Kα radiation (λ=1.5406/1.5444 Å) with a Ni filter at 40 kV and 40 mA. Diffraction data were collected over a 2θ range of 5–40°, with a step size of 0.1°, to identify the crystalline structures of the zeolitic supports. All powder samples were loaded on PMMA holders.

Catalyst Preparation.

$La(BH_4)_3(THF)_3$. $La(BH_4)_3(THF)_3$ was synthesized via the reported method.[1-3] $LaCl_3$ (2.46 g, 10.0 mmol) and excess sodium borohydride (1.52 g, 40.1 mmol) were heated at reflux in THF for 5 d. Cannula filtration of the solution removed the residual $NaBH_4$ and NaCl. The filtrate was then evaporated under vacuum, giving a solid residue that was extracted with toluene. The extracts were concentrated and then cooled to –30 °C, yielding $La(BH_4)_3(THF)_3$ (3.10 g, 7.75 mmol, 77.4%) as a colorless powder that was isolated and stored under N_2 in a glovebox. The ^1H and ^{11}B NMR spectra and DRIFTS matched the literature values. ^1H NMR (toluene-d_8, 400 MHz, 25 °C): δ 1.35 (t, 12 H, THF-CH_2), 1.73 (br q, 12 H, $^1J_{BH}$ = 80 Hz, BH_4), 3.82 (t, 12 H, THF-OCH_2). ^{11}B NMR (toluene-d_8, 400 MHz, 25 °C): δ 19.0 (p, $^1J_{BH}$ = 85 Hz, BH_4). IR (DRIFTS, cm^{-1}): 3100-2850 (m, ν_{CH}) 2450 (s, $\nu_{BH\text{-terminal}}$) 2250-2050 (m, $\nu_{BH\text{-bridging}}$).

Dealuminated HY_{30} (**DA-HY_{30}**). The dealuminated HY_{30} (DA-HY_{30}) zeolite was synthesized following the reported method.[4, 5] HY_{30} (1 g) was mixed with 13 M nitric acid (20 mL) with vigorous stirring, and this mixture was heated at reflux (100 °C) for 20 h. The solid was isolated by filtration and then washed with deionized water (500 mL × 7) until the washings were pH 7. The white solid powder was dried at 100 °C overnight, calcined at 500 °C for 5 h under flowing air, and then dehydroxylated by heating at 500 °C for 5 h at 10^{-4} Torr. The Si/Al ratio of DA-HY_{30} was 123.5 ± 1.3 (ICP-OES). Characterization data for DA-HY_{30}: powder X-ray diffraction (Figure S1), N_2 physisorption/BET analysis (Table S1), and DRIFTS (Figure S2).

R_3Si-HY. The zeolite (0.300 g) and chlorotriphenylsilane (0.3 mmol) were mixed in pentane (5.0 mL). The mixture was stirred at room temperature for 24 h. The supernatant was decanted, the solid was washed with pentane (3 × 10 mL), and the isolated silylated faujasite material was dried under dynamic vacuum (10^{-4} mbar) at room temperature for 24 h. The DRIFTS spectra of Ph_3Si-HY_{30}, Ph_3Si-HY_{250}, or Ph_3Si-DA-HY_{30}, Ph_3Si-HY_{15} and Ph_3Si-HY_{50} products are shown in Figure S2. A similar procedure was used for silylation of HY_{30} with different sized silanes including $Ph_2MeSiCl$ and Me_3SiCl with same loading (1.0 mmol/g). The DRIFTS spectra of Ph_2MeSi-HY_{30} and Me_3Si-HY_{30} are shown in Figure S2. To cap all OH groups on HY_{250} and SiO_2, excess loading of Me_3Si-NMe_2 (2.5 mmol/g) was applied for sillylation (Figure S6).

$La(BH_4)_2(THF)_2/Ph_3Si$-HY_{30} (**La/Ph_3Si-HY_{30}**). A toluene solution of $La(BH_4)_3(THF)_3$ (0.040 g, 0.10 mmol, 10 mL) was added to Ph_3Si-HY_{30} (0.350 g). The mixture was stirred at room temperature for 20 h. The supernatant was decanted, the solid was washed with toluene (3 × 10 mL), and the material was dried under dynamic vacuum (10^{-4} mbar) at room temperature for 24 h. This procedure was also used to synthesize La/Ph_3Si-HY_{250}, La/Me_3Si-HY_{250}, La/DA-HY_{30}, and La/Ph_3Si-DA-HY_{30}. The isolated materials were characterized by DRIFTS (Figures S2 and S3), and La loading was determined by ICP-OES (see Tables 2 and S3).

PXRD Patterns of HY_{30}, DA-HY_{30} and Dehydroxylated DA-HY_{30}.

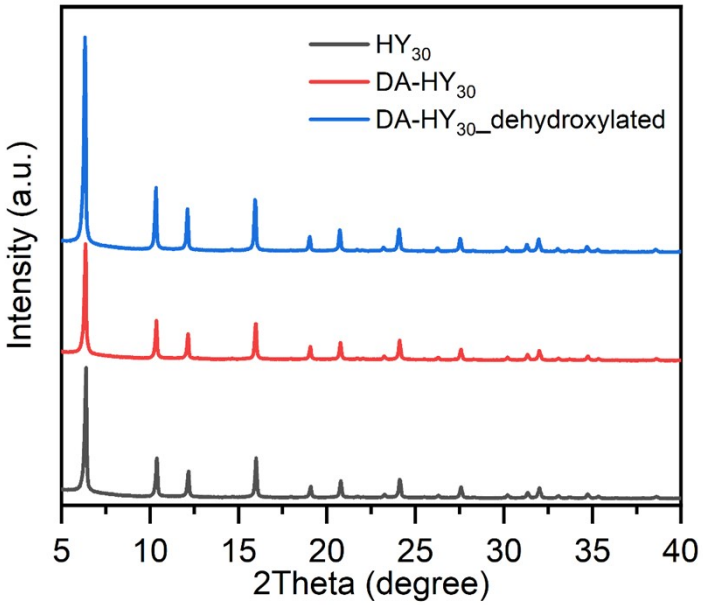

Figure S1. XRD patterns of HY_{30}, DA-HY_{30} and dehydroxylated DA-HY_{30}.

Physical Properties of Materials

Table S1. Surface and porosity information of HY_{30}, Ph_3Si-HY_{30}, DA-HY_{30}, Ph_3Si-DA-HY_{30} obtained from N_2 physisorption measurement.

	V_{total} [a] (cm^3/g)	$V_{micropore}$ [b] (cm^3/g)	$S_{BET\ total}$ [c] (m^2/g)	$S_{external}$ [b] (m^2/g)
HY_{30}	0.54	0.30	708	83
Ph_3Si-HY_{30}	0.50	0.30	668	66
DA-HY_{30}	0.48	0.19	662	246
Ph_3Si-DA-HY_{30}	0.40	0.17	540	167

[a]single point total pore volume at relative pressure = 0.99; [b]t-plot method; [c]BET surface area.

Table S2. OH loadings in supports determined by quantification of toluene formation upon reaction with $Mg(Bn)_2(dioxane)_2$.

Support	**OH amounts (mmol/g)**
HY_{30}	0.86
Ph_3Si-HY_{30}	0.45
Ph_3Si-HY_{250}	0.39
Me_3Si-HY_{250}	0.10
DA-HY_{30}	0.91
Ph_3Si-DA-HY_{30}	0.68
SiO_2	0.66

Table S3. Weight percentage of La, and molar ratio of Si/Al and B/La in different catalysts.

Catalysts	La (wt%)	Molar ratio of Si/Al	Molar ratio of B/La
La/HY_{30}	1.2 ± 0.2	30.2 ± 1.1	2.9 ± 0.4
La/Ph_3Si-HY_{30}	0.9 ± 0.2	31.9 ± 1.7	3.1 ± 1.1
La/Ph_3Si-HY_{250}	1.1 ± 0.1	259 ± 6.7	2.5 ± 0.4
La/Me_3Si-HY_{250}	0.5 ± 0.1	317 ± 7.8	3.3 ± 0.5
La/DA-HY_{30}	1.3 ± 0.3	121 ± 5.1	2.7 ± 0.3
La/Ph_3Si-DA-HY_{30}	1.0 ± 0.2	136 ± 4.9	2.9 ± 0.7

Infrared Spectra.

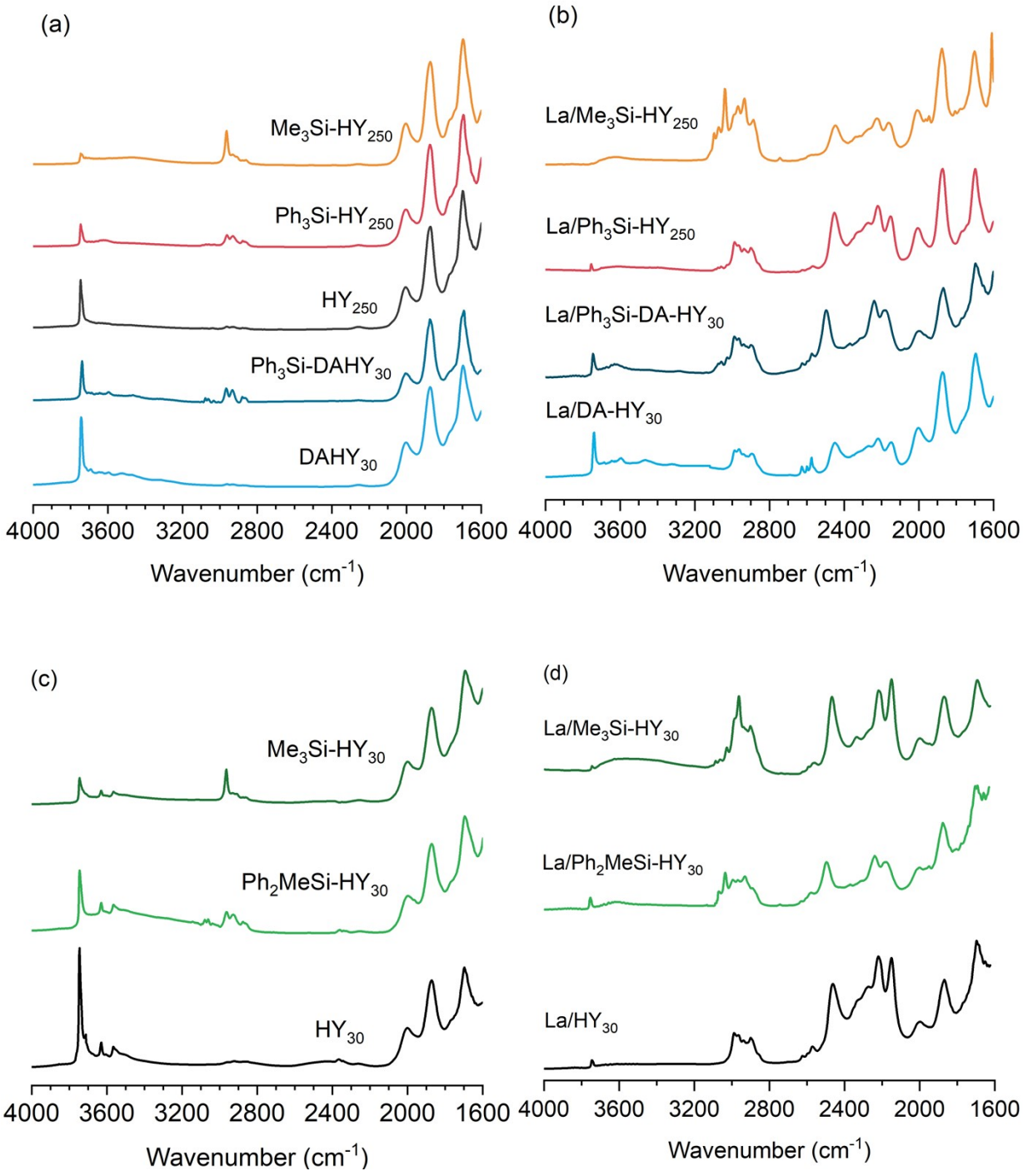

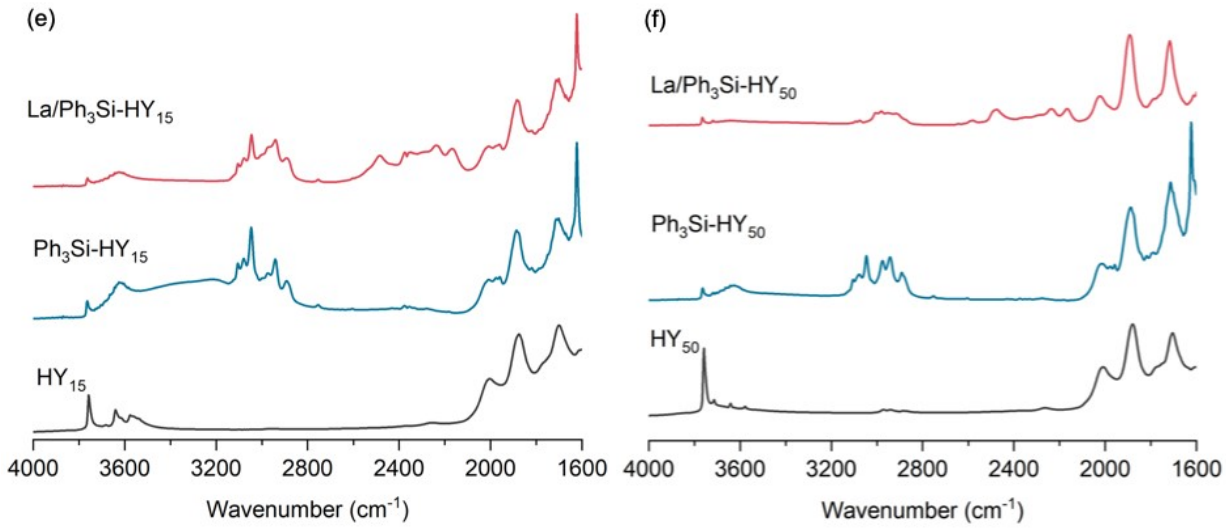

Figure S2. DRIFTS spectra of supports (a) DA-HY_{30}, Ph_3Si-DA-HY_{30}, HY_{250}, Ph_3Si-HY_{250}, Me_3Si-HY_{250}; (b) La-grafted precatalysts La/DA-HY_{30}, La/Ph_3Si-DA-HY_{30}, La/Ph_3Si-HY_{250}, La/Me_3Si-HY_{250}; (c) supports Ph_2MeSi-HY_{30}, Me_3Si-HY_{30} compared to parent batch of HY_{30}; (d) La-grafted precatalysts La/Ph_2MeSi-HY_{30}, La/$PhMe_2Si$-HY_{30}, La/Me_3Si-HY_{30} compared to La/HY_{30}; (e) HY_{15}, Ph_3Si-HY_{15}, La/Ph_3Si-HY_{15} and (f) HY_{50}, Ph_3Si-HY_{50}, La/Ph_3Si-HY_{50}.

Molecular sizes of four silanes for sillylation.

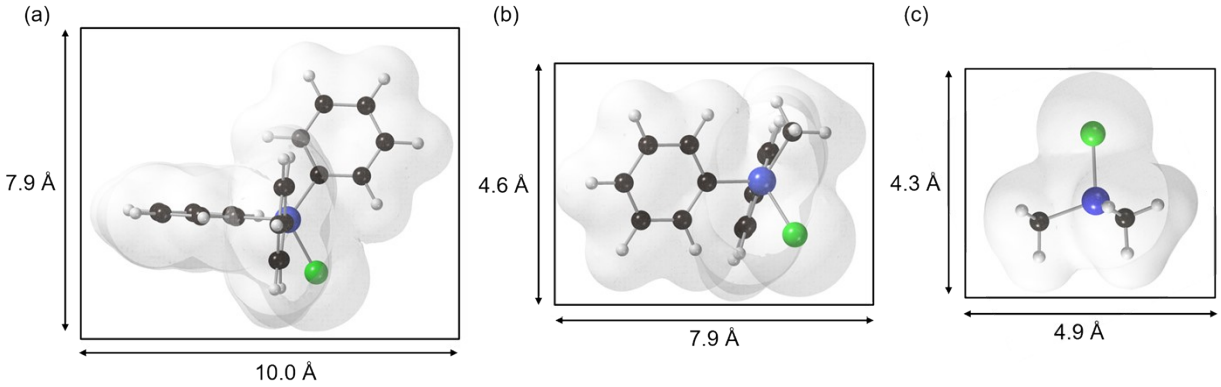

Figure S3. The roughly estimated molecular size of (a) Ph_3SiCl (10.0 x 10.0 x 7.9 Å), (b) $Ph_2MeSiCl$ (9.5 x 7.9 x 4.6 Å) and (c) Me_3SiCl (4.9 x 4.9 x 4.3 Å). Molecular structures are optimized by DFT calculation and are applied Van der Waals force surface.

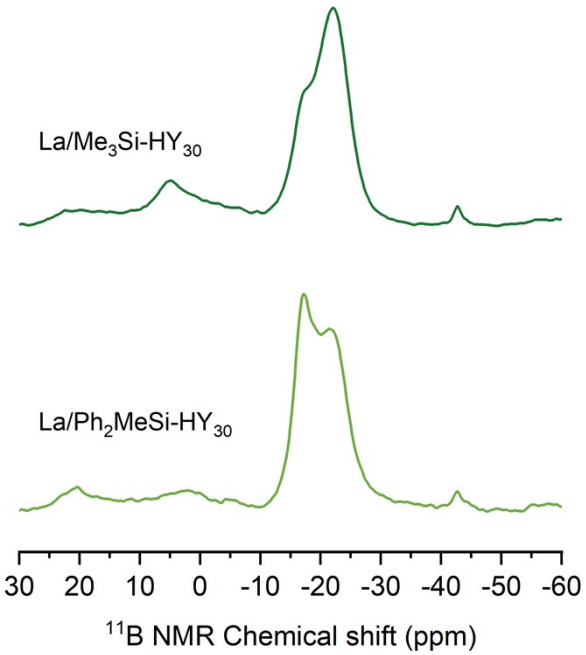

Figure S4. Solid-state ^{11}B NMR spectra of La/Ph_2MeSi-HY_{30} and La/Me_3Si-HY_{30} (from bottom to top).

Catalytic Borylation Experiments.

Catalyst testing. In a typical experiment, an air-tight, Teflon-valved, re-sealable glass reactor was charged with the precatalyst (~0.002 mmol La, 0.025 g, see Table 2), benzene (0.50 mL), and HBpin (0.15 mL, 1.0 mmol) in the glovebox. The reaction vessel was sealed and then heated in an aluminum block at 120 °C for 12 h. The reaction mixture was cooled, the solution was separated from the solid catalyst, and then the solution-phase of reaction mixture was characterized by calibrated GC-MS and ^{11}B NMR spectroscopy. Each experiment was repeated at least two times.

Product analysis. The yield of PhBpin in the above experiments was determined using calibrated GC-MS. An aliquot of the reaction solution (0.100 g) was withdrawn and mixed with TMOB in benzene (100 mM, 0.20 mL). This mixture was then diluted to 1.0 mL solution by adding benzene. Quantification was achieved using external calibration with TMOB. A calibration curve for quantifying PhBpin was constructed by plotting the molar amount of PhBpin as a function of the ratio of peak area between PhBpin and TMOB to obtain the response factor (RF). The amount of PhBpin obtained with the calibration curve, using the following equation:

$$Molar\ amount\ of\ PhBpin = \frac{Peak\ Area\ (PhBpin)}{Peak\ Area\ (TMOB)} \times RF \times \frac{weight\ (total\ reaction\ mixture)}{weight\ (withdrawn\ reaction\ mixture)}$$

The conversion of HBpin was monitored with solution ^{1}H and ^{11}B NMR spectroscopy. Typically, 0.100 g of reaction solution was mixed with 0.4 mL benzene-d_6, and NMR spectra were acquired. The recycle delay (rd) to obtain quantitative ^{11}B NMR spectra is 2 s. Yield and selectivity of PhBpin were calculated with respect to HBpin. Specifically, the yield of PhBpin was calculated by dividing PhBpin moles by initial HBpin moles, and selectivity of PhBpin was calculated by dividing yield of PhBpin by conversion of HBpin. The production of PhBpin was confirmed using ^{11}B NMR spectroscopy by spiking the reaction solution with authentic PhBpin.

Molecular Dynamics Simulation with Machine-Learning.

Training of the machine-learning (ML) potentials was performed using the DeePMD framework and codes.[6] DFT calculations are carried out using the PBE functional[7] and the VASP code[8, 9] with plane-wave basis sets with a 400 eV energy cutoff. For a system of seven elements (Al, B, C, H, La, O, and Si), a total of 127 subsystems, include 7 single elements, 21 binary, 35 triple, ..., of subsystems are considered. For each subsystem, DFT simulations, typically at a temperature of 1600 K, are performed. An iterative procedure of training and generating data is implemented, with results of MD simulations using machine learned potential used as starting points of further DFT simulations.

Due to the large number of elements involved, we use a light version of the ML potentials trained on DFT data for a subsystem up to a density $1.5m\rho c/M$, where m is the number of atomic species, $M = 7$ is the total number of species, and ρc is a cutoff density of the subsystem. For example, for the CHO subsystem, $m = 3$, and $\rho c = 2.5$ g/cm^3, so that the maximum density in the training data involving CHO is 1.6 g/cm3. While we don't expect this ML potential to be good for the pure C system, it is adequate for the general system as long as no single for a few elements dominate the whole system.

The $La(BH_4)_2(THF)_2$ in HY_{30} zeolite system is also simulated by DFT for 1 ps at various temperatures. About half of the results are used in the trainings, and the other half are used for validation. A total of 598 individual DFT MD simulations (each one up to 2000 time steps) using VASP[8, 9] was used to train the DeePMD potential (with se_e2_a descriptor). For efficiency, we use a single Γ point for the k-point grid, and 0.2 eV Gaussian smearing of the electron occupancy, with no spin polarization.

Structure of La Complex Immobilized on Silica

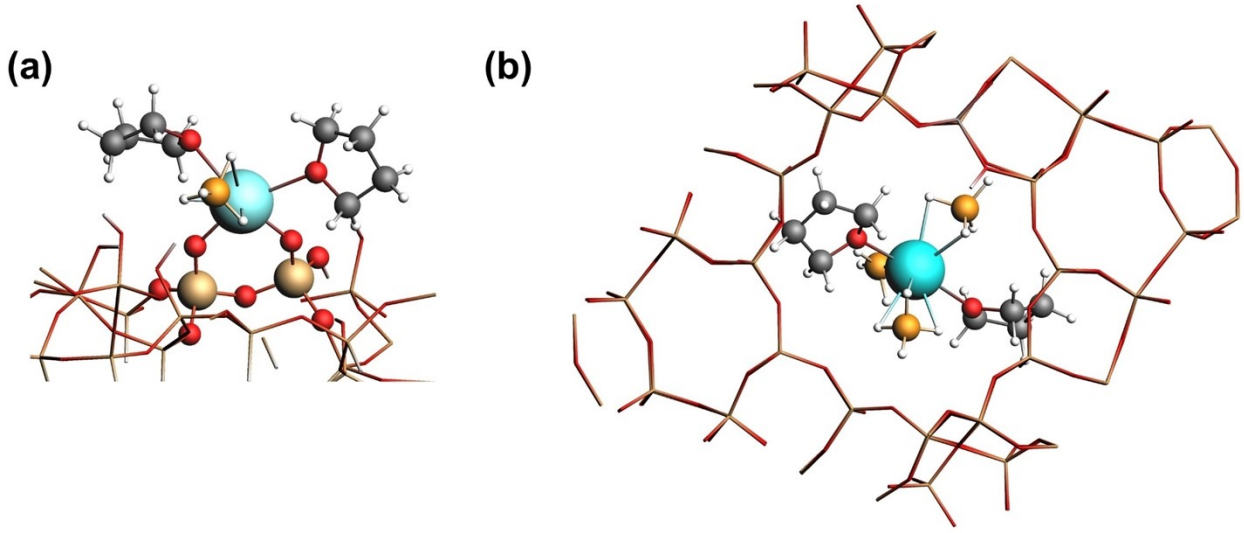

Figure S5. DFT-optimized structures of La complex immobilized on silica surface in bipodal configurations (a) and physisorbed in zeolite supercage (b). White, grey, red, orange, green, beige, and light blue spheres represent hydrogen, carbon, oxygen, boron, aluminum, silicon, and lanthanum atoms, respectively.

Table S4. Experimentally and theoretically estimated NMR line shape parameters.

Species	Figure		δ	δ_{iso} (ppm)	C_Q (MHz)	η_Q	[a)] P_Q (MHz)	[a)] δ_{QIS} (ppm)
B2	4b	exp.	-23.0	-21.3			1.4	-1.7
La@silica (monopodal)	4c	calc.	-23.7 [b)]	-22.7	1.06	0.16	1.06	-1.00
La@silica (bipodal)	S3a	calc.	-30.7 [b)]	-30.1	0.82	0.27	0.83	-0.62
La, physisorbed	S3b	calc.	-22.5[b)]	-21.1	1.25	0.11	1.25	-1.40

a) $\delta_{QIS}\,(ppm) = 3/17\ \ [4S(S+1) - 3]/[4S(2S-1)]^2 \cdot \left(P_Q^2/\nu_0^2\right) \cdot 10^6$, $P_Q \equiv C_Q\sqrt{1+\eta_Q^2/3}$, where S is the spin quantum number of the nucleus, P_Q is the second order quadrupolar effect, ν_0 is the Larmor frequency of the nucleus, C_Q is the quadrupolar coupling constant, η_Q is the quadrupolar asymmetry parameter. b) $\delta = \delta_{iso} + \delta_{QIS}$.

$La(BH_4)_3(THF)_3$ Physiosorbed on Supports

The protonated sites (OH groups) on two supports Me_3Si-SiO_2 and Me_3Si-HY_{250} were fully capped by the silylating agent (Me_3Si-NMe_2 with excess loading 10mmol/g).[10] DRIFTS of the samples are shown in Figure S4. $La(BH_4)_3(THF)_3$ (~0.010 g) and the internal standard tetrakis(trimethylsilyl)silane (TMSS, 0.008 g, 0.025 mmol) were dissolved in benzene-d_6 (0.8 mL). The solution was mixed with Me_3Si-SiO_2 (0.022 g) or Me_3Si-HY_{250} (0.027 g) in an NMR tube at room temperature for 30 h (Figure S5). ^{1}H NMR spectra of the lanthanum precursor solution before and after mixing with the supports were measured and normalized to the integral for TMSS signal at 0.26 ppm (chemical shift reference to benzene-d_6 at 7.15 ppm). The signal intensity of $La(BH_4)_3(THF)_3$ is equivalent before and after mixing with Me_3Si-SiO_2. The mixed solids were filtered, washed with benzene (4 × 5 mL), and dried under vacuum. The loading of La on La/Me_3Si-SiO_2 was determined by ICP-OES to be 0.017±0.008 mmol/g.

The signal for BH_4 decreased by ~0.0030 mmol in a mixture of $La(BH_4)_3(THF)_3$ and Me_3Si-HY_{250}, corresponding to 0.0010 mmol $La(BH_4)_3(THF)_3$ adsorbed on Me_3Si-HY_{250}. The signal for THF reduced by only 0.0022 mmol. The larger amount of THF than BH_4 in solution demonstrates that ~0.0008 mmol of THF is dissociated from the ~0.001 mmol of La precursor encapsulated in Me_3Si-HY_{250}, corresponding to approximately one equivalent of THF per adsorbed La complex. 0.031±0.010 mmol/g of La in La/Me_3Si-HY_{250} was determined by ICP-OES.

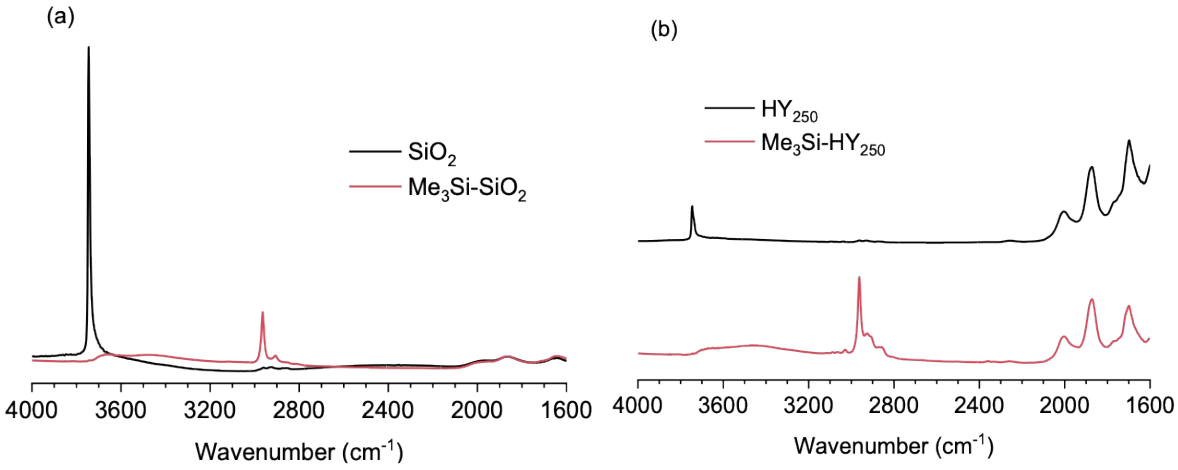

Figure S6. (a) DRIFTS spectra of SiO_2 (black line) and Me_3Si-SiO_2 (red line); (b) DRIFTS spectra of HY_{250} (black line) and Me_3Si-HY_{250} (red line).

^{1}H NMR Spectra Analyzing of Grafting of $La(BH_3)_3(THF)_3$

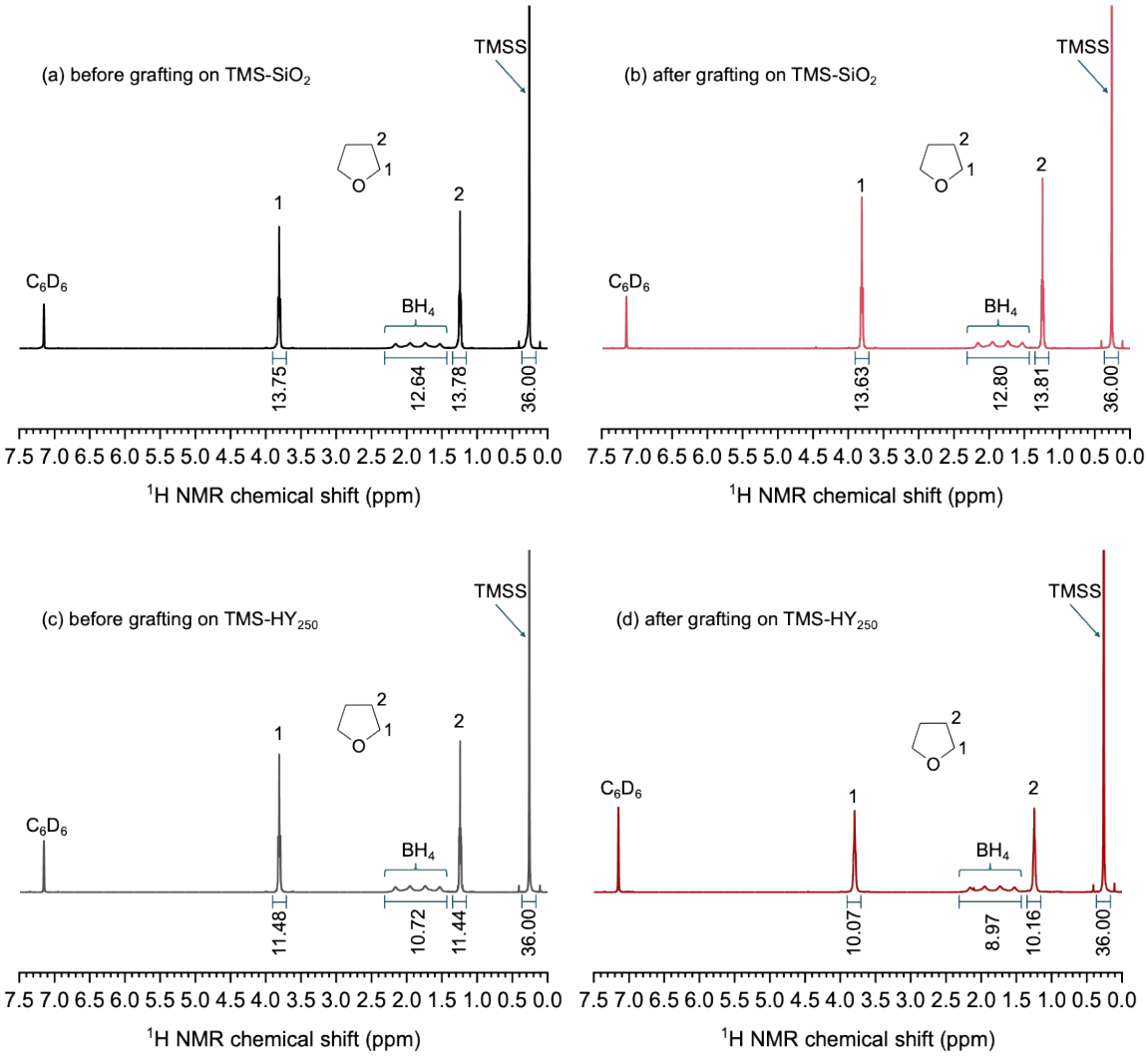

Figure S7. Spectra (a) and (b) are ^{1}H NMR measurements of $La(BH_3)_3(THF)_3$ in benzene-d_6 (reference at 7.15 ppm) before and after mixing with Me_3Si-SiO_2, respectively; spectra (c) and (d) are ^{1}H NMR measurements of $La(BH_3)_3(THF)_3$ in benzene-d_6 before and after mixing with Me_3Si-HY_{250}, respectively. The signal at 0.26 ppm is the internal TMSS standard. Signals at 1.23 and 3.80 ppm are THF in La complexes and quadruplet from 1.6-2.1 ppm is BH_4 in the La complex.

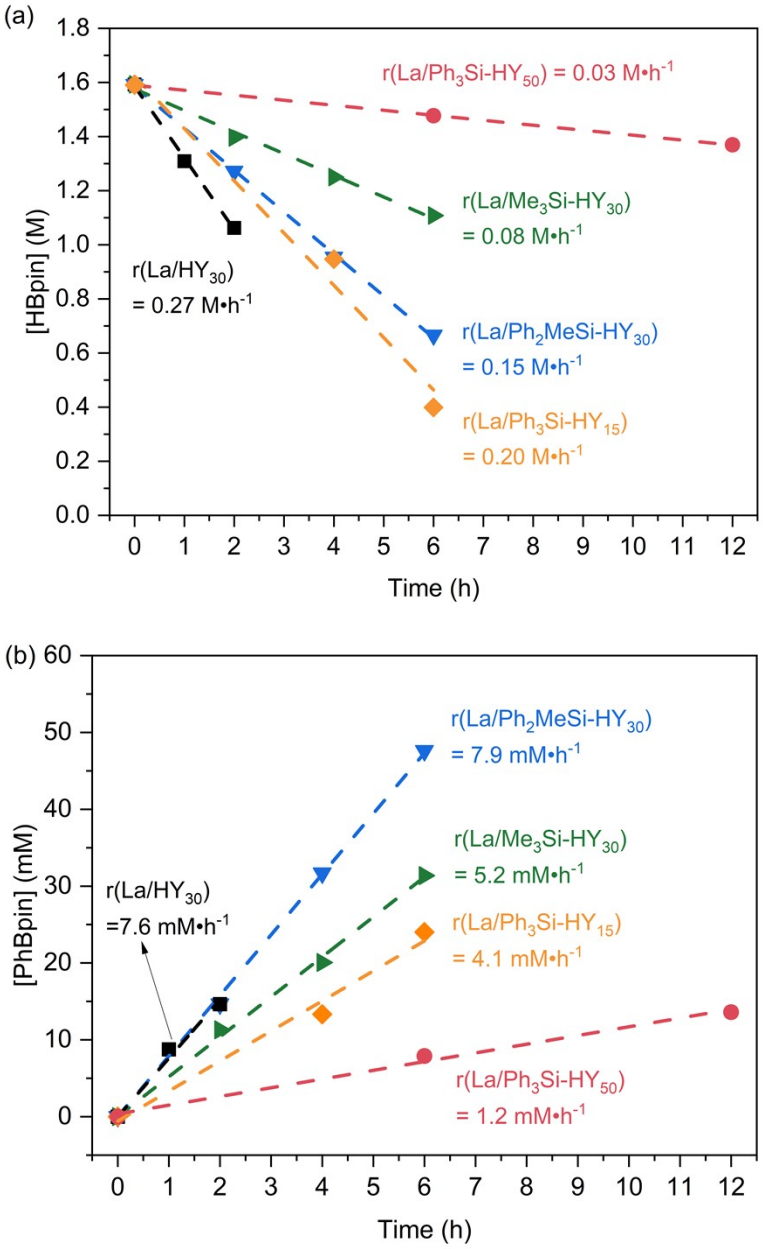

Figure S8. Initial rates of HBpin conversion (a) and PhBpin formation (b) from benzene borylation catalyzed by La/HY_{30} (black square), La/Ph_2MeSi-HY_{30} (blue down arrow), La/Me_3Si-HY_{30} (green right arrow), La/Ph_3Si-HY_{15} (orange diamond) and La/Ph_3Si-HY_{50} (red circle) were obtained by plotting [HBpin] and [PhBpin] as a function of time, respectively.

References

1. M. Mostajeran, E. Ye, S. Desgreniers and R. T. Baker, Base-Metal Nanoparticle-Catalyzed hydrogen release from ammine yttrium and lanthanum borohydrides, *Chem. Mater.*, 2017, **29**, 742-751.
2. S. M. Guillaume, M. Schappacher and A. Soum, Polymerization of ε-Caprolactone Initiated by Nd(BH4)3(THF)3: Synthesis of Hydroxytelechelic Poly(ε-caprolactone), *Macromol.*, 2003, **36**, 54-60.
3. N. Ajellal, G. Durieux, L. Delevoye, G. Tricot, C. Dujardin, C. M. Thomas and R. M. Gauvin, Polymerization of Racemic β-butyrolactone Using Supported Catalysts: A Simple Access to Isotactic Polymers, *Chem. Commun.*, 2010, **46**, 1032-1034.
4. W. L. Dai, S. S. Zhang, Z. Y. Yu, T. T. Yan, G. J. Wu, N. J. Guan and L. D. Li, Zeolite Structural Confinement Effects Enhance One-pot Catalytic Conversion of Ethanol to Butadiene, *ACS Catal.*, 2017, **7**, 3703-3706.
5. L. Qi, Y. F. Zhang, M. A. Conrad, C. K. Russell, J. Miller and A. T. Bell, Ethanol Conversion to Butadiene over Isolated Zinc and Yttrium Sites Grafted onto Dealuminated Beta Zeolite, *J. Am. Chem. Soc.*, 2020, **142**, 14674-14687.
6. L. F. Zhang, J. Q. Han, H. Wang, R. Car and E. Weinan, Deep Potential Molecular Dynamics: A Scalable Model with the Accuracy of Quantum Mechanics, *Phys. Rev. Lett.*, 2018, **120**.
7. J. P. Perdew, K. Burke and M. Ernzerhof, Generalized Gradient Approximation Made Simple, *Phys. Rev. Lett.*, 1997, **78**, 1396-1396.
8. G. Kresse and J. Furthmuller, Efficient Iterative Schemes for Ab Initio Total-Energy Calculations Using a Plane-Wave Basis Set, *Phys. Rev. B*, 1996, **54**, 11169-11186.
9. G. Kresse and J. Furthmuller, Efficiency of Ab-Initio Total Energy Calculations for Metals and Semiconductors Using a Plane-Wave Basis set, *Comp. Mater. Sci.*, 1996, **6**, 15-50.
10. R. L. Brutchey, D. A. Ruddy, L. K. Andersen and T. D. Tilley, Influence of Surface Modification of Ti-SBA15 Catalysts on the Epoxidation Mechanism for Cyclohexene with Aqueous Hydrogen Peroxide, *Langmuir*, 2005, **21**, 9576-9583.